Dual-Readout of the Mechanical Response of a bis-Acridinium [2]Rotaxane

Johnny Hu, Sonia Adrouche, Etienne S. Gauthier, Christophe Gourlaouen, Nolwenn Le Breton, Marco Cecchini, Sylvie Choua, Valérie Heitz, Henri-Pierre Jacquot de Rouville

Chemistry
A European
Journal

Chemistry Europe
European Chemical Societies Publishing

Accepted Article

Title: Dual-Readout of the Mechanical Response of a bis-Acridinium [2]Rotaxane

Authors: Johnny Hu, Sonia Adrouche, Etienne S Gauthier, Nolwenn Le Breton, Marco Cecchini, Christophe Gourlaouen, Sylvie Choua, Valérie Heitz, and Henri-Pierre Jacquot de Rouville

To be cited as: *Chem. Eur. J.* **2022**, e202202840

Link to VoR: https://doi.org/10.1002/chem.202202840

WILEY-VCH

10.1002/chem.202202840

WILEY-VCH

RESEARCH ARTICLE

Dual-Readout of the Mechanical Response of a bis-Acridinium [2]Rotaxane

Johnny Hu,[a] Sonia Adrouche,[a] Etienne S. Gauthier,[a] Nolwenn Le Breton,[a] Marco Cecchini,[a] Christophe Gourlaouen,[a] Sylvie Choua,[a] Valérie Heitz*[a] and Henri-Pierre Jacquot de Rouville*[a]

[a] J. Hu, S. Adrouche, Dr. E. S. Gauthier, Dr. N. Le Breton, Dr. M. Cecchini, Dr. C. Gourlaouen, Dr. S. Choua, Prof. V. Heitz, Dr. H.-P. Jacquot de Rouville
Institut de Chimie de Strasbourg
LSAMM, POMAM and IFM research groups
CNRS UMR 7177
4, rue Blaise Pascal
67000 Strasbourg, France.
E-mail: v.heitz@unistra.fr, hpjacquot@unistra.fr

Supporting information for this article is given via a link at the end of the document.

Abstract: A [2]rotaxane built around a multi-responsive bis-acridinium macrocycle has been synthesized. Structural investigation has confirmed the interlocked nature of the molecule and MD simulations illuminated its conformational dynamics with atomic resolution. Both halochromic and redox switching properties were explored to shed light on the mechanical responses and electronic changes that occur in the bis-acridinium [2]rotaxane. The topology of the rotaxane led to different mechanical behaviors, upon addition of hydroxide ions or reduction, easily detected by UV/Vis spectroscopy and electrochemistry.

Introduction

The mechanical bond[1] has brought new perspectives in supramolecular chemistry.[2] Whereas dynamic host-guest assemblies are stabilized by weak interactions, the mechanical bond ensures a kinetic and a thermodynamic stabilization in mechanically interlocked molecules (MIMs),[3] among which catenanes and rotaxanes can be cited. They opened the way to functional devices such as artificial molecular machines, molecular-scale logic gates, and functional supramolecular biomaterials.[4] The controlled motion of the subcomponents in [2]rotaxanes is essential to mimic biomolecular machines. As a consequence, the development of new supramolecular building blocks experiencing large and reversible geometrical and electronic changes upon a chemical, redox or photonic stimulus is of primary importance to reach more complex systems.[5] One way to complexity goes through the use of orthogonal stimuli but the additional stimulus is often used for the readout of the mechanical response.[6] Rare are the examples involving orthogonal stimuli to trigger different mechanical responses.[7] Indeed, the design of such systems is challenging since they typically require the combination of compatible molecular switches in the same architecture.[8]

The acridinium unit is a π-extended electro-deficient aromatic moiety able to recognize electron-rich aromatic guests through π-donor/ π-acceptor interactions.[9] In addition, this aromatic moiety is an attractive building block in supramolecular chemistry since its electronic properties and shape can be drastically changed upon reduction or addition of nucleophiles.[10] Despite this unique multi-responsive behaviour, the acridinium core was not intensively used in supramolecular chemistry and was barely incorporated in MIMs.[11] For instance, W. Abraham and his group have developed [2]rotaxanes incorporating a crown ether macrocycle with a pending acridinium unit.[12,13] In these examples, the acridinium motif was not used as a recognition unit specific to π-π stacking interactions.

We recently developed a 35-atom macrocycle (**M35^{2+}**) consisting of two cofacial acridinium units linked by a rigid 3,5-dipyridylanisole and a flexible alkenyl spacer.[14] In this cyclophane, the switching properties of the acridinium units were also advantageously exploited to tune the binding affinity for polycyclic aromatic hydrocarbons. Upon reduction, the di-reduced macrocycle (**M35^{0}**) revealed a strongly decreased binding constant for perylene (**Per**, K_a from 1200 to 54 L mol^{-1} in $C_2H_4Cl_2$) while upon addition of hydroxide ions, no affinity was observed. In other words, both stimuli led to the dissociation of the host-guest system.

In contrast, it was envisioned that the enhanced kinetic inertness and thermodynamic stability provided by a rotaxane architecture would be of interest in differentiating the mode of action of both stimuli in **M35^{2+}**. It is foreseen that the halochromic and redox properties will thus give rise to a multi-readout of the motion in the system. Herein, the design and the synthesis of a [2]rotaxane incorporating the multi-responsive bis-acridinium macrocycle **M35^{2+}** is reported. Its interlocked nature was explored by 1D variable temperature and 2D NMR experiments while its conformational dynamics by all-atom Molecular Dynamics simulations. Finally, the multi-responsive properties of the MIM were probed upon addition of hydroxide ions and upon reduction. The halochromic properties were followed by ^{1}H NMR and UV/Vis spectroscopies and the redox properties were studied by electrochemical techniques (UV/Vis spectroelectrochemistry, cyclic and differential pulse voltammetry), EPR experiments and DFT calculations.

Results and Discussion

Design and Binding Study with Pyrene. Pyrene (**Pyr**) was considered as an interaction site for the bis-acridinium macrocycle **M35·2PF$_6$** in a MIM since its regio-functionalized

10.1002/chem.202202840

derivatives are commercially available in comparison to **Per** which usually requires tedious stepwise recrystallization.[15] Followed by ^{1}H NMR spectroscopy, binding experiments revealed a K_a of 328 ± 3 L mol^{-1} between the bis-acridinium macrocycle **M35·2PF$_6$** and **Pyr** in CD_3CN (see SI, Figure S4.1-S4.3). In addition, a clipping strategy was considered for the formation of the [2]rotaxane and the synthesis of a methylated bis-acridinium tweezer was performed (see structure Figure 1a and see SI, section 3). A complexation study between this tweezer and **Pyr** revealed a K_a of 191 ± 5 L mol^{-1} in CD_3CN (Figure S4.4-S4.6). Despite the degrees of freedom in the tweezer leading to different conformers in solution, **Pyr** appears to be a suitable interaction site for the synthesis of the [2]rotaxane.[16] The interaction between the tweezer and **Pyr** was rationalized by X-ray diffraction analysis of the corresponding methylated bis-acridinium tweezer (Figure 1b-c).[17] In the crystalline state, the system exhibits a U-shape conformation. In addition, a suitable distance between the two acridinium moieties ($d_{C9\text{-}C9}$ = 7.190(4) Å and $d_{N\text{-}N}$ = 7.492(4) Å) was found for π-stacking interactions with an aromatic guest.

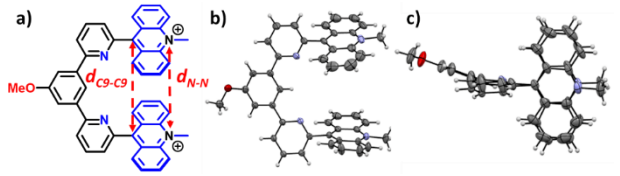

Figure 1. a) Scheme of the methylated bis-acridinium tweezer, b) side view and c) top view of the crystal structure of methylated bis-acridinium tweezer (thermal ellipsoids at 50% probability level; PF_6^- anions have been omitted for clarity).

Synthesis. The synthesis of the [2]rotaxane **1·2PF$_6$** was performed according to a clipping strategy (Scheme 1). First, the synthesis of the dumbbell **2** involved the formation of a tetraarylmethane stopper **3** bearing six tert-butyl functional groups and a terminal alkyne functional group. This synthesis was carried out following Gibson synthetic strategy.[18] Compound **3** (2.0 equiv.) was reacted with 1,6-diiodopyrene[19] (1.0 equiv.) under Sonogashira conditions in a 1:1 THF/piperidine (v/v) mixture of solvents using $Pd(PPh_3)_4$ (10 mol%) and CuI (10 mol%) as catalysts. The dumbbell **2** was isolated in 90% yield. Finally, the [2]rotaxane **1·2PF$_6$** was obtained by reacting the dumbbell **2** (1.0 equiv.) with the bis-acridinium tweezer **4·2(CF$_3$COO)** (1.3 equiv.)[14] in the presence of Grubbs(I) catalyst in CH_2Cl_2 (50 mol%). After anion metathesis and purification, the rotaxane **1·2PF$_6$** was obtained in 18% yield as a trans/cis mixture of isomers of olefines (7:3 ratio).

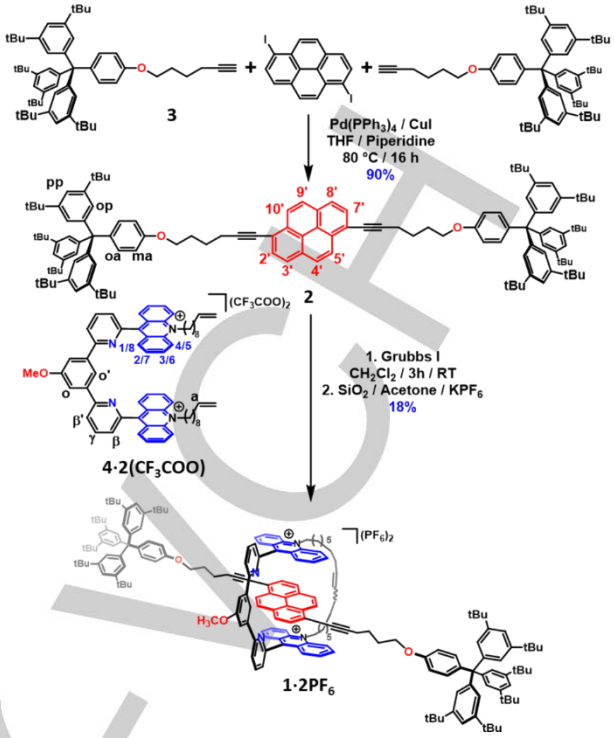

Scheme 1. Synthesis of the [2]rotaxane **1·2PF$_6$** according to a clipping strategy.

Structural Characterizations. The structure of the rotaxane **1·2PF$_6$** was confirmed by NMR spectroscopy (1D and 2D) as well as by mass spectrometry. After anion exchange, the comparison of the ^{1}H NMR spectrum of **1·2(CF$_3$COO)** in $CDCl_3$ and its isolated components (Figure 2), namely the free macrocycle **M35·2(CF$_3$COO)** and dumbbell **2**, revealed upfield shifts of the acridinium ($\Delta\delta(H_{1/8})$ = –0.31, $\Delta\delta(H_{2/7})$ = –0.15, $\Delta\delta(H_{3/6})$ = –0.64 and $\Delta\delta(H_{4/5})$ = –1.65 ppm) and the pyrene protons ($\Delta\delta(H_{4'/9'})$ = –0.88, $\Delta\delta(H_{2'/7'})$ = –0.70 and $\Delta\delta(H_{3'/8'\text{-}5'/10'})$ = –0.94 ppm).[20] In contrast, the inner proton of the cavity of the macrocycle ($\Delta\delta(H_{o'})$ = +0.83 ppm) and the olefinic protons ($\Delta\delta(H_a)$ = +0.38 ppm) exhibited a downfield shift. These observations reflect the reciprocal influence of the anisotropy effects of pyrene and **M35·2(CF$_3$COO)**. The mechanically interlocked nature of the [2]rotaxane **1·2PF$_6$** was unambiguously confirmed by NOESY and DOSY experiments. Through space correlations between the $H_{4'/9'\text{-}2'/7'}$ pyrene protons of the dumbbell and the $H_{o'}$ proton of the macrocycle were monitored (see SI, Figure S3.31-S3.32) and all protons of **1·2PF$_6$** exhibited the same diffusion (D = 485 µm² s^{-1}, Figure S3.37). Finally, no dethreading was detected upon heating a solution of **1·2PF$_6$** in CD_3CN at 353 K for 16 h (Figure S3.25) thus showing the efficiency of the stoppers. Mass spectrometry also revealed the presence of the interlocked molecule in the gas phase. A peak corresponding to the molecular ion **[1]$^{2+}$** was observed at *m/z* 1284.8587 (Figure S3.38). It is worthwhile to note that the fluorescence of pyrene was quenched in **1·2PF$_6$** compared to **2** indicating the spatial proximity of the electron rich pyrene and the acridinium units (Figure S3.40).

10.1002/chem.202202840

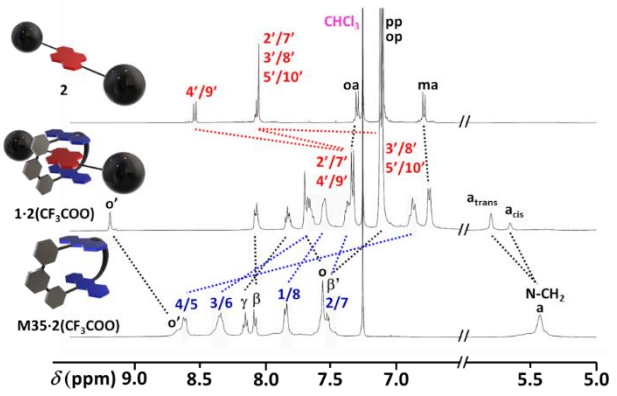

Figure 2. ^{1}H NMR spectra (500 MHz, $CDCl_3$, 298 K, c = 5 × 10^{-3} mol L^{-1}) stack of a) the dumbbell **2**, b) the [2]rotaxane **1·2(CF₃COO)** and c) the macrocycle **M35·2(CF₃COO)** (zoom aromatic region).

Surprisingly, **1·2PF₆** showed a good solubility in various solvents and the ^{1}H NMR spectra of **1·2PF₆** were similar when recorded in CD_3OD, CD_3CN, [D_6]acetone, [D_7]DMF and CD_2Cl_2 (see SI, Figure S3.26). This observation indicates that the macrocycle mainly resides at the vicinity of the pyrene core. This hypothesis was confirmed by variable temperature experiments in CD_3CN at 343 K with no changes of the proton chemical shifts of the [2]rotaxane (Figure S3.28). Interestingly, the ^{1}H NMR spectrum at 193 K in [D_6]acetone showed two sets of signals corresponding to the $H_{o'}$ proton of the macrocycle ($\delta(H_{o'})$ = 9.45 and 9.39 ppm) in a 6:4 ratio suggesting two stable positions of the pyrene core in the cavity of the macrocycle or two conformers of **M35²⁺** (Figure S3.27).

In order to explore the conformational dynamics of the MIM in solution, molecular dynamics (MD) simulations were performed on the corresponding [2]pseudo-rotaxane in a box of CH_3CN at 298 K (Figure S9.1). The existence of (at least) two conformational states of the MIM (called here "centered" and right tilted "dx") in a reversible equilibrium was observed (Figure 3 and see SI, Figure S9.2). These distinct states are the result of a slight tilting of the pyrene moiety within the cavity of the macrocycle. In other words, the interaction pattern (see short contacts represented as yellowish dashed line in Figure 3) between the central carbon atom of the macrocycle (C7 in red linked to $H_{o'}$) and the three labelled carbon atoms of the pyrene core (C13 in green, C14 in purple and C18 in cyan) changes over time. These two representative structures show that the chemical environment of the $H_{o'}$ proton changes on account of the position of pyrene sitting in the cavity of the macrocycle thus rationalizing the ^{1}H NMR at variable temperature.

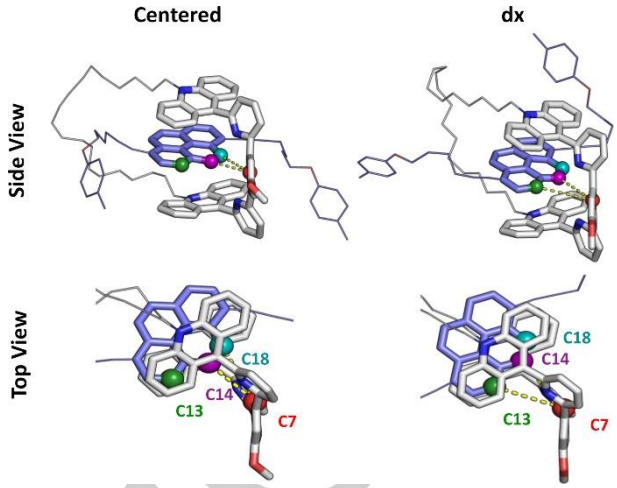

Figure 3. Main conformational states of the [2]pseudo-rotaxane identified by MD simulations. In the "centered" conformation, the central carbon of the bis-acridinium units (C7) is in contact with two aromatic carbons on the same pyrene ring (C14 and C18). In the "dx" conformation, C7 is in contact with carbons belonging to two different pyrene rings (C13 and C14). Only the acridinium and pyrene moieties are visualized. See ESI for details.

Acid-Base Study. The acid-base switching properties of the bis-acridinium rotaxane **1·2PF₆** were explored. Addition of hydroxide ions to a solution of **1·2PF₆** quantitively led to the corresponding bis-acridane derivative **5**. Dearomatization of the acridinium core was confirmed by UV/Vis spectroscopy (Figure 4). In CH_2Cl_2, the acridinium centered $\pi\rightarrow\pi^*$ transitions at 350 nm (ε = 25 000 L mol^{-1} cm^{-1}) and 435 nm (8 000) were not observed in the spectrum of **5** and a new transition was monitored at 320 nm (15 000).[21] Full reversibility of the conversion of the acridane rotaxane **5** to the acridinium rotaxane **1·2PF₆** was demonstrated under acidic conditions. Addition of a small amount of TFA (2 equiv.) restored the spectrum of **1²⁺** on account of the rearomatization of the acridinium cores. Fatigue studies showed no loss of reactivity upon successive addition of TFA and TBAOH thus demonstrating the robustness of the interlocked system. Interestingly, analysis of a solution of **5** by mass spectrometry showed peaks at m/z 2588.72, 2602.73, 2619.72 and 2633.74 corresponding to the molecular ions **[5–OH]⁺**, **[5]⁺**, **[5–OH+OCH₃]⁺** and **[5–2OH+2OCH₃]⁺** (Figure S3.55). This observation confirms the scrambling of the nucleophile of the bis-acridane rotaxane under these conditions as already seen in this family of compounds.[14]

10.1002/chem.202202840

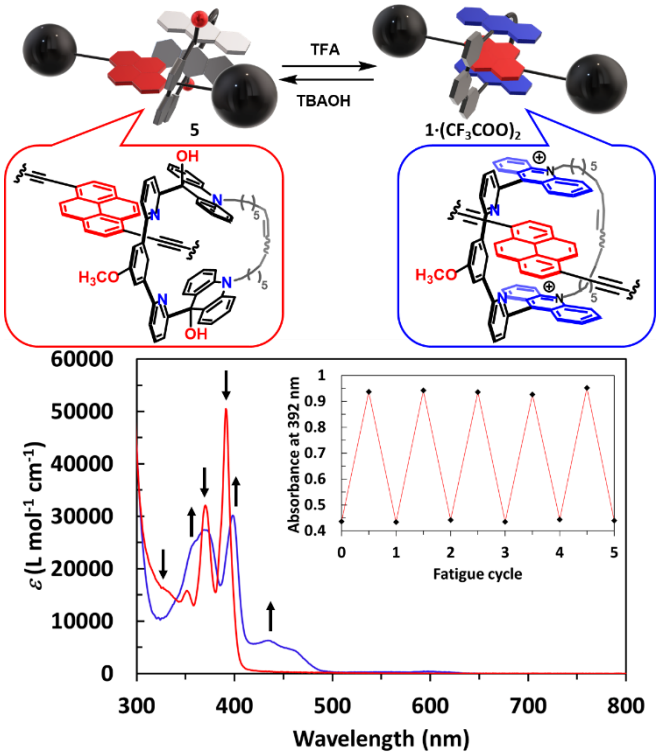

Figure 4. UV/Vis (CH_2Cl_2, l = 0.1 cm, 298 K) spectra overlay of a solution of **5** ($c = 1.5 \times 10^{-5}$ mol L^{-1}) before (red) and after addition of TFA (2 equiv., blue). Inset: Fatigue study monitored by UV/Vis spectroscopy at 392 nm. Each cycle corresponds to the successive addition of TBAOH (16 equiv.) followed by addition of TFA (18 equiv.).

Compared to the ^{1}H NMR spectrum of **1·2PF$_6$** (see SI, Figure S5.1), the ^{1}H NMR spectrum of **5** showed an upfield shift of the acridane with respect to the acridinium protons ($\Delta\delta(H_{1/8})$ = –0.21, $\Delta\delta(H_{2/7})$ = –0.62, $\Delta\delta(H_{3/6})$ = –0.64 and $\Delta\delta(H_{4/5})$ = –0.13 ppm). Closer scrutiny to the spectrum revealed a downfield shift of the pyrene protons ($\Delta\delta(H_{4'/9'})$ = –0.37, $\Delta\delta(H_{2'/7'})$ = –0.32 and $\Delta\delta(H_{3'/8'\text{-}5'/10'})$ = –0.45 ppm).[22] The shift difference between the bis-acridane rotaxane **5** and the isolated dumbbell are less pronounced than that of the bis-acridinium rotaxane **1·2PF$_6$** except for the H_{ma} proton ($\Delta\delta(H_{ma})$ = –0.13 ppm in **5** *vs.* –0.05 in **1·2PF$_6$**, Table S1). This observation suggests that the macrocycle moves away from the pyrene core upon addition of hydroxide ions. Interestingly, two sets of signals were monitored at 233 K for the H_{ma} proton of the stoppers (Figure S3.52). In other words, the macrocycle comes closer to the phenoxy groups of the dumbbell at low temperature resulting in two different environments for the stoppers. Consequently, the spectrum of **5** at 298 K reflects an average conformation coming from the constant shuttling of the macrocycle along the axle. It thus shows that the motion in the [2]rotaxane can be reversibly triggered by addition/removal of hydroxide ions.

Molecular dynamics simulations of the bis-acridane rotaxane **5** fully support the shuttling of the macrocycle along the axle (Figure 5a). During a 100-ns trajectory at 353 K, the macrocycle appears to reside successively in between the central pyrene moiety and either stopper of the dumbbell **2** for about 25 ns before crossing it and moving to the other side, as reflected by the variation of the distances (d_1 and d_2) between the $C_{o'}$ carbon of the macrocycle and the central quaternary carbons of the stoppers (Figure 5b, top). In sharp contrast, no shuttling of the macrocycle was detected in simulations carried out at 233 K (Figure 5b, bottom). The simulation results are in good agreement with the NMR spectra of **5** and explain the frozen motion detected by variable temperature ^{1}H NMR at low temperature.

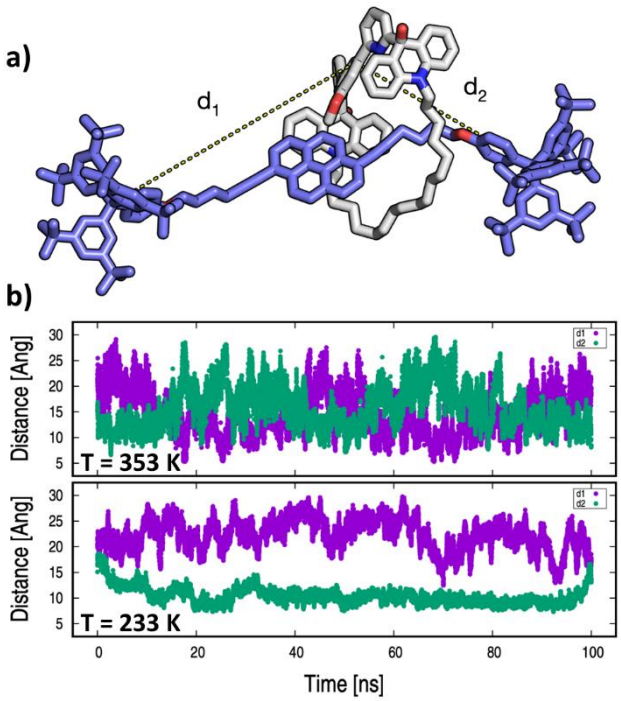

Figure 5. Molecular dynamics simulations of the bis-acridane rotaxane **5**. a) Representative snapshot of the rotaxane with the interatomic distances used to monitor the shuttling of the macrocycle. The shuttling distances (d_1 and d_2) were measured between the $C_{o'}$ of the macrocycle and the central quaternary carbons of the stoppers. b) Time series of the shuttling distances at high (top) and low (bottom) temperature over 100 ns MD.

In other words, the motion can be easily detected by UV/Vis spectroscopy at 435 nm. It is worthwhile to note that the rotaxane **5** exhibits a regain of luminescence properties on account of the conversion of the acridinium cores to the corresponding acridane moieties (Figure S3.40). This variation in the visible region of the spectrum can be seen as a first ON/OFF readout of the motion in the system.

Electrochemical Study. Electrochemical studies were performed to probe the electronic interactions stabilizing the bis-acridinium macrocycle on pyrene and to investigate the potential motion of the macrocycle upon reduction of the acridinium units. In DMF, two reduction peaks (E_{c1} = –0.970 V and E_{c2} = –1.790 V *vs.* SCE) and one concomitant reoxidation peak (E_{a1} = –0.880 V *vs.* SCE) were observed by cyclic voltammetry experiments (Figure 6a). The first reduction process exhibits a quasi-reversible behavior as suggested by the observed peak potential difference ($\Delta E = |E_{a1} - E_{c1}|$ = 90 mV). The plot of the cathodic and anodic intensity as a function of the square root of the scan rate (I_c and $I_a = f(\nu^{1/2})$) shows a linear relationship underlying a process under diffusion control (see SI, Figure S6.3). In addition, UV/Vis spectroelectrochemical (SEC) experiments unambiguously

10.1002/chem.202202840

confirmed a bi-electronic reduction for this first reduction process (Figure S6.4).[10] Indeed, formation of **1⁰** (E_{app} = –1.0 V *vs.* SCE) revealed the characteristic spectrum of the acridinium radical species showing two maxima at 464 (ε = 5 000 L mol^{-1} cm^{-1}) and 533 nm (4 200) with the simultaneous decrease of the typical acridinium centered $\pi\rightarrow\pi^*$ transitions at 435 (8 000) and 454 nm (4 500). It is worthwhile to note that the full restoration of the spectrum of **1·2PF$_6$** occurred upon re-oxidation thus corroborating the clean chemical reversibility of this electrochemical process (Figure S6.5). The second reduction peak is irreversible and affects the intensity of the reoxidation process (I_a decreasing) as it is often seen in acridinium derivatives. This behavior is the result of a well-known EEC mechanism (electron-electron-chemical) for this family of compounds.[9b, 23] Interestingly, a cathodic shift in potential for both reduction waves in **1·2PF$_6$** was observed ($\Delta(E_{1/2}^{(1)})$ = –47 mV and $\Delta(E_{c2})$ = –40 mV vs SCE) in comparison to the isolated macrocycle **M35·2PF$_6$** (Figure 6a). Indeed, pyrene enriches the acridinium units of the macrocycle making them harder to reduce. In other words, these shifts suggest that no shuttling takes place upon reduction of **1·2PF$_6$** since no alternative stable positions exist.[7a, 24]

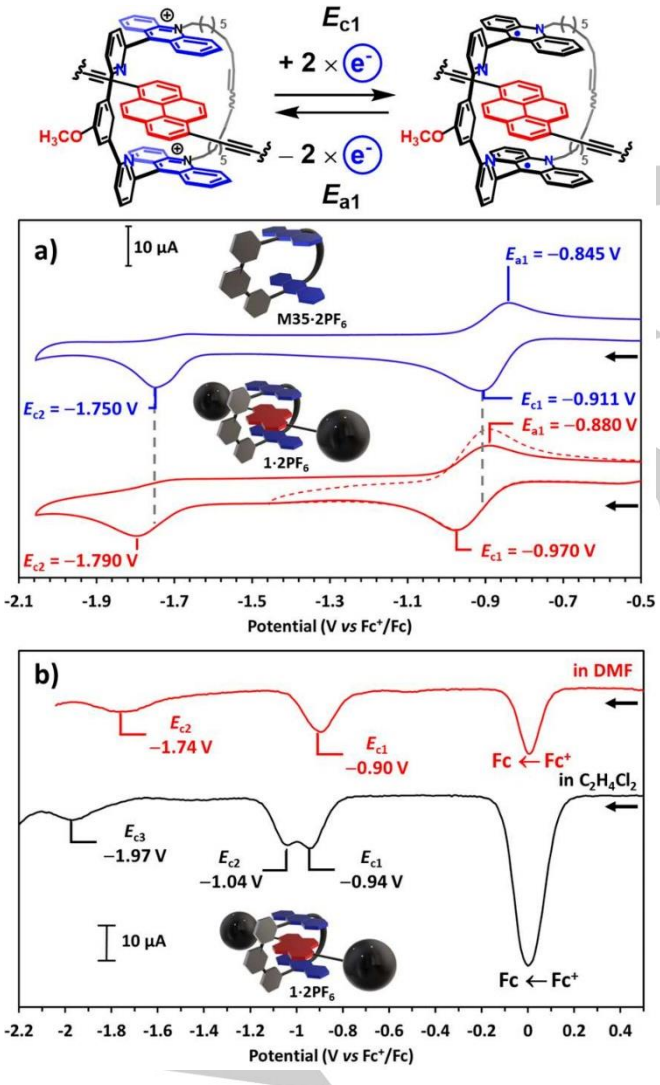

Figure 6. a) Cyclic voltammograms (DMF, WE: Pt, CE: Pt, RE: Hg/Hg$_2$Cl$_2$, 100 mV s^{-1}) of a solution (c = 1 × 10^{-3} mol L^{-1}) of bis-acridinium macrocycle (blue) **M35·2PF$_6$** and **1·2PF$_6$** (red). b) Square wave voltammograms of **1·2PF$_6$** in DMF (red) and in $C_2H_4Cl_2$ (black) in the presence of one equivalent of Ferrocene (Fc).

When cyclic voltammetry experiments were performed in 1,2-dichloroethane ($C_2H_4Cl_2$), a different behavior was observed. Instead of the first bi-electronic reduction process observed in DMF, two quasi-reversible reduction events (E_{c1} = –0.940 V and E_{c2} = –1.04 V *vs* SCE) were monitored (Figure 6b and see SI, Figure S6.7-S6.9). UV/Vis SEC experiments in $C_2H_4Cl_2$ (Figure S6.10-S6.11) suggest a sequential reduction of the acridinium units in **1·2PF$_6$**. Interestingly, this behavior was not observed for the isolated macrocycle **M35·2PF$_6$**[14] and can be attributed to a charge solvation effect. In contrast, the bis-acridane rotaxane **5** does not exhibit any electrochemical response within the same range of potential (Figure S6.14). The difference of the electrochemical responses between **1·2PF$_6$** and **5** can be seen as a direct ON/OFF readout of the dynamic behavior within the [2]rotaxane. This detection is ensured by the reversible geometrical and electronic changes of the same recognition unit, here the acridinium fragment.

EPR Study. In order to shed light on the reduction state of the rotaxane, continuous wave electron paramagnetic resonance (EPR) experiments were undertaken in $C_2H_4Cl_2$ (c = 5 × 10^{-4} mol L^{-1}). EPR spectra were recorded at 260 K upon addition of a reducing agent (cobaltocene, Co(C$_5$H$_5$)$_2$) to generate the reduced species. The EPR spectrum of the 10-(dec-9-en-1-yl)-9-phenylacridinium hexafluorophosphate model compound displayed well resolved hyperfine coupling constants (see simulation in SI, Figure S7.1) whereas a single line was observed for the monoreduced macrocycle (**M35$^{+/\bullet}$**, Figure 7). Consequently, this observation indicates the existence of an intramolecular electron exchange reaction leading to a line broadening effect on the EPR spectrum.[25] Surprisingly, the presence of pyrene in **1$^{+/\bullet}$** restored a partially resolved spectrum reflecting a decreased spin exchange interaction.

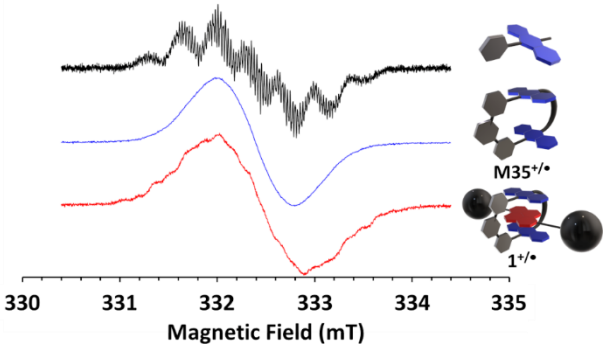

Figure 7. X-band EPR spectra of a solution ($C_2H_4Cl_2$, 260 K, c = 5 × 10^{-4} mol L^{-1}) of the 10-(dec-9-en-1-yl)-9-phenylacridinium hexafluorophosphate model compound (black line, with a modulation amplitude 0.1 mT at a frequency of 30 kHz; microwave power of 1 mW), of **M35·2PF$_6$** (blue line, with a modulation amplitude 0.1 mT at a frequency of 100 kHz; microwave power of 1 mW) and of **1·2PF$_6$** (red line, with a modulation amplitude 0.1 mT at a frequency of 100 kHz; microwave power of 1 mW) in the presence of Co(C$_5$H$_5$)$_2$ (0.8 equiv.).

DFT calculations were undertaken in order to rationalize the EPR spectra. The monoreduced macrocycle **M35$^{+/\bullet}$** and rotaxane **1$^{+/\bullet}$** have their SOMO localized on one of the acridinium units as

10.1002/chem.202202840

expected (Figure 8). Interestingly, a flattening of the structure in **M35$^{+/\bullet}$** is observed with a distance of ≈ 3.5 Å between the reduced acridinium and the second acridinium fragment (Figure 8a). This interaction is comparable to the formation of an intramolecular π-mer between both interacting units. It is worthwhile to note that the existence of acridinium π-mers seems to be corroborated by the EPR concentration study on the 10-(dec-9-en-1-yl)-9-phenylacridinium hexafluorophosphate model compound (see SI, Figure S7.3).[23] In comparison, the structural rearrangement of the macrocycle is prevented in the monoreduced rotaxane **1$^{+/\bullet}$** on account of the presence of pyrene (Figure 8b). The distance between the reduced acridinium and the second acridinium fragment was found to be ≈ 7 Å thus explaining the decrease of the spin exchange in the rotaxane **1$^{+/\bullet}$** (Figure 7a).

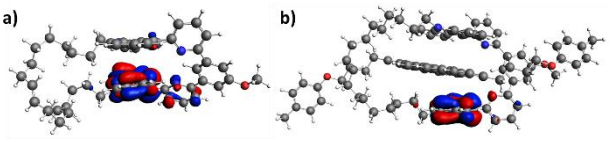

Figure 8. DFT calculations (B3LYP functional) showing the optimized geometry and the SOMO orbital of a) the monoreduced macrocycle **M35$^{+/\bullet}$** and b) monoreduced rotaxane **1$^{+/\bullet}$**.

Conclusion

In summary, we have reported on the synthesis, the structural characterization and the conformational dynamics of a novel [2]rotaxane incorporating a bis-acridinium macrocycle. In addition, the halochromic properties of the acridinium units were exploited to set in motion the macrocycle and the dumbbell relative to each other in the [2]rotaxane. The redox properties of the [2]rotaxane were explored and revealed a kinetic stabilization of the assembly compared to its subcomponents. To the best of our knowledge, this is a rare example of mechanically interlocked molecule responsive to orthogonal stimuli on a same recognition unit, namely the acridinium core, leading to two distinct mechanical responses with a direct ON/OFF readout assessed by UV/Vis spectroscopy and electrochemistry. In addition, EPR studies coupled to a DFT investigation showed that after monoelectronic reduction, a spin exchange interaction is observed but decreased in comparison to the isolated macrocycle. This behavior is likely the result of a prevented π-mer formation in the MIM on account of the presence of the pyrene core. This work opens the way to the use of the acridinium core as a recognition unit for radical templation through π-mer formation.

Acknowledgements

This work was supported by the CNRS and the University of Strasbourg. We gratefully acknowledge the International Center for Frontier Research in Chemistry FRC (http://www.icfrc.fr) and LabEx CSC for a PhD fellowship to SA and the INC of the CNRS (Emergence@INC21 program) for financial support. We are grateful to the Fédération de Chimie Le Bel FR 2010 of the University of Strasbourg. Calculations were carried at the Strasbourg computing center (HPC). JH thanks the French Ministry of National Education for a PhD Fellowship. Prof. Jean-Pierre Launay and Dr. Romain Ruppert are thanked for fruitful discussions.

Keywords: Supramolecular Chemistry • Rotaxane • Orthogonal Stimuli • Dual-Readout • Acridinium

[1] a) M. A. Olson, Y. Y. Botros and J. F. Stoddart, *Pure Appl. Chem.* **2010**, *82*, 1569–1574; b) C. J. Bruns and J. F. Stoddart, The Nature of the Mechanical Bond: From Molecules to Machines, Wiley, New Jersey, **2016**.

[2] a) D. J. Cram and J. M. Cram, *Science* **1974**, *183*, 803–809; b) J.-M. Lehn, *Science*, **1985**, *227*, 849–856; c) J.-M. Lehn, *Angew. Chem., Int. Ed. Engl.* **1990**, *29*, 1304–1319; d) J.-M. Lehn, Supramolecular Chemistry: Concepts and Perspectives;Wiley-VCH: New York, NY, **1995**; e) J. Rebek Jr, *Chem. Soc. Rev.* **1996**, *25*, 255–264; f) J. M. Spruell, *Pure Appl. Chem.* **2010**, *82*, 2281–2294.

[3] a) E. Wasserman, *J. Am. Chem. Soc.* **1960**, *82*, 4433–4434; b) J. F. Stoddart, *Angew. Chem. Int. Ed.* **2017**, *56*, 11094–11125; c) J.-P. Sauvage, *Angew. Chem. Int. Ed.* **2017**, *56*, 11080–11093.

[4] a) J.-M. Lehn, *Angew. Chem. Int. Ed.* **2013**, *52*, 2836–2850; b) M. W. Ambrogio, C. R. Thomas, Y.-L. Zhao, J. I. Zink, J. F. Stoddart, *Acc. Chem. Res.* **2011**, 903–913; c) B. Feringa, *Angew. Chem. Int. Ed.* **2017**, *56*, 11060–11078; d) L. van Dijk, M. J. Tilby, R. Szpera, O. A. Smith, H. A. P. Bunce, S. P. Fletcher, *Nat. Rev. Chem.* **2018**, *2*, 0117; e) A. P. DaSilva, N. D. McClenaghan, *Chem. Eur. J.* **2004**, *10*, 574–586; f) O. J. G. Goor, S. I. S. Hendrikse, P. Y. W. Dankers, E. W. Meijer, *Chem. Soc. Rev.*, **2017**, *46*, 6621–6637.

[5] H.-Y. Zhou, Q.-S. Zong, Y. Han, C.-F. Chen, *Chem. Commun.* **2020**, *56*, 9916–9936.

[6] H. Li, J.-N. Zhang, W. Zhou, H. Zhang, Q. Zhang, D.-H. Qu, H. Tian, *Org. Lett.* **2013**, *15*, 3070–3073.

[7] a) E. Córdova, R. A. Bissell, N. Spencer, P. R. Ashton, J. F. Stoddart, A. E. Kaifer, *J. Org. Chem.* **1993**, *58*, 6550–6552; b) R. A. Bissell, E. Cordova, A. E. Kaifer, J. Fraser Stoddart, *Nature*, **1994**, *369*, 133–137; c) T. Avellini, H. Li, A. Coskun, G. Barin, A. Trabolsi, A. N. Basuray, S. K. Dey, A. Credi, S. Silvi, J. F. Stoddart, M. Venturi, *Angew. Chem., Int. Ed.*, **2012**, *51*, 1611−1615.

[8] a) M. Jeong, J. Park, S. Kwon, *Eur. J. Org. Chem.* **2020**, 7254–7283; b) M. Baroncini, S. Silvi, A. Credi, *Chem. Rev.*, **2020**, *120*, 200−268.

[9] a) S. Claude, J.-M. Lehn, F. Schmidt, J.-P. Vigneron, *J. Chem. Soc. Chem. Commun.* **1991**, 1182–1185; b) H.-P. Jacquot de Rouville, J. Hu, V. Heitz, *ChemPlusChem* **2021**, *86*, 110–129 and references therein.

[10] a) K. Kano, B. Zhou, S. Hashimoto, *Chem. Lett.* **1985**, 791–792; b) A. Gosset, Z. Xu, F. Maurel, L.-M. Chamoreau, S. Nowak, G. Vives, C. Perruchot, V. Heitz, H.-P. Jacquot de Rouville, *New J. Chem.* **2018**, *42*, 4728–4734.

[11] a) K. Yazaki, Y. Sei, M. Akita, M. Yoshizawa, *Chem. Eur. J.* **2016**, *22*, 17557–17561; b) K. Kurihara, K. Yazaki, M. Akita, M. Yoshizawa, *Angew. Chem. Int. Ed.* **2017**, *56*, 11360–11364.

[12] a) M. Orda-Zgadzaj, W. Abraham, *Synthesis* **2007**, *21*, 3345–3356; b) M. Orda-Zgadzaj, W. Abraham, *Tetrahedron* **2008**, *64*, 2669–2676.

[13] a) W. Abraham, K. Buck, M. Orda-Zgadzaj, S. Schmidt-Schäffer, U.-W. Grummt, *Chem. Commun.* **2007**, 3094–3096; b) W. Abraham, A. Wlosnewski, K. Buck, S. Jacob, *Org. Biomol. Chem.* **2009**, *7*, 142–154; c) A. Vetter, W. Abraham, *Org. Biomol. Chem.* **2010**, *8*, 4666–4681; d) Y. Duo, S. Jacob, W. Abraham, *Org. Biomol. Chem.* **2011**, *9*, 3549–3559.

[14] J. Hu, J. S. Ward, A. Chaumont, K. Rissanen, J.-M. Vincent, V. Heitz, H.-P. Jacquot de Rouville, *Angew. Chem. Int. Ed.* **2020**, *59*, 23206–23212.

[15] K. Hayashi, M. Inouye, *Eur. J. Org. Chem.* **2017**, 4334–4337.

[16] M. Inouye, K. Hayashi, Y. Yonenaga, T. Itou, K. Fujimoto, T.-A. Uchida, M. Iwamura, K. Nozaki, *Angew. Chem. Int. Ed.* **2014**, *53*, 14392–14396.

[17] Crystal data for methylated bis-acridinium tweezer: $C_{45}H_{34}N_4O{\cdot}2(PF_6)$, yellow plate, crystal size 0.200 × 0.200 × 0.120 mm, monoclinic, space group C 2/c, a = 20.5217(9) Å, b = 14.9440(6) Å, c = 28.7482(11) Å, α = 90°, β = 108.472(2)°, γ = 90°, V = 8362.2(6) Å^3, Z = 8, ρ_{calc} = 1.488, T = 120(2) K, $R_1(F^2 > 2\sigma F^2)$ = 0.0935, wR2 = 0.2665. Out of 196052 reflection a total of 10422 were unique. Crystallographic data (excluding structure factors) for the structures reported in this communication have

been deposited with the Cambridge Crystallographic Data Center as supplementary publication no. CCDC–2195137.

[18] The Grignard reagent obtained from the commercially available 1-bromo-3,5-di-tert-butylbenzene was reacted with methyl 3,5-di-tert-butylbenzoate in THF at 60°C. The resulting tris(3,5-di-tert-butylphenyl)methanol (**6**) was isolated in 72% yield. Conversion of compound **6** in the presence of a large excess of phenol under acidic conditions led to 4-(tris(3,5-di-tert-butylphenyl)methyl)phenol (**7**) in 93% yield. (see: H. W. Gibson, S.-H. Lee, P. T. Engen, P. Lecavalier, J. Sze, Y. X. Shen, M. Bheda, *J. Org. Chem.* **1993**, *58*, 3748–3756). Compound **7** was functionalized with the tosylated pent-4-yn-1-ol in the presence of K_2CO_3 acting as a base in DMF. After purification using column chromatography, compound **3** was obtained in 88% yield (see SI).

[19] 1,6-diiodopyrene was obtained from the commercially available 1,6-dibromopyrene under Cu(I) catalyzed Finkelstein conditions (see: H. Abe, Y. Mawatari, H. Teraoka, K. Fujimoto, M. Inouye, *J. Org. Chem.* **2004**, *69*, 495–504). It is worthwhile to note that reaction between 1,6-dibromopyrene and compound **3** under Sonogashira conditions led to dumbbell **2** in 25% yield.

[20] It is worthwhile to note that the macrocycle **M35^{2+}** is poorly soluble in $CDCl_3$ as a PF_6^- salt. In consequence, a counter-ion exchange from PF_6^- to CF_3COO^- had to be performed to allow solubilization of both **1·2(CF$_3$COO)** and **M35·2(CF$_3$COO)** and a direct comparison of their corresponding ^{1}H NMR spectra in $CDCl_3$.

[21] All electronic transitions were rationalized by DFT calculations and are in good agreement with the experimental data (see SI, Figure S8.2, S8.3 and S8.5).

[22] Upon heating a solution of **5** in $CDCl_3$ for 16 h, no dethreading experiments was monitored (Figure S3.51). DOSY experiments also confirmed the interlocked nature of **5** with the presence of a single diffusing species (D = 361 µm² s^{-1}, see Figure S3.57).

[23] W. Koper, S. A. Jonker, J. W. Verhoeven, *Recl. Trav. Chim. Pays-Bas* **1985**, *104*, 296–301.

[24] In addition, no opening of a hysteresis loop was observed thus confirming that no shuttling occurred (see: H.-P. Jacquot de Rouville, J. Iehl, C. J. Bruns, P. L. McGrier, M. Frasconi, A. A. Sarjeant, J. Fraser Stoddart, *Org. Lett.* **2012**, *14*, 5188–5191).

[25] This behavior is similar to the behavior observed by Stoddart and coworkers with bluebox, see: A. Trabolsi, N. Khashab, A. C. Fahrenbach, D. C. Friedman, M. T. Colvin, K. K. Cotí, D. Benítez, E. Tkatchouk, J.-C. Olsen, M. E. Belowich, R. Carmielli, H. A. Khatib, W. A. Goddard, M. R. Wasielewski, J. F. Stoddart, *Nat. Chem.* **2010**, *2*, 42–49.

10.1002/chem.202202840

WILEY-VCH

RESEARCH ARTICLE

Entry for the Table of Contents

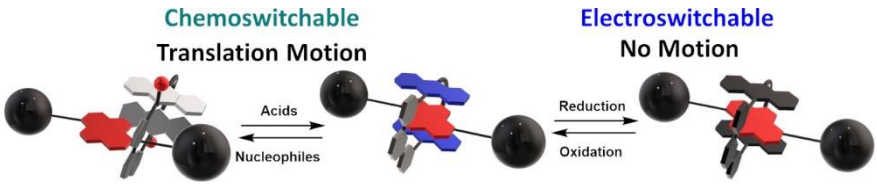

The chemochromic and electrochemical properties of a switchable bis-acridinium [2]rotaxane lead to two different mechanical responses and an ON/OFF reading of the motion in the assembly.

Institute and/or researcher Twitter usernames: @Heitz_group, @HPJdeRouville